JOURNAL OF GEOPHYSICAL RESEARCH, VOL. 106, NO. A12, PAGES 29,373–29,385, DECEMBER 1, 2001

# Anisotropic magnetosheath: Comparison of theory with Wind observations near the stagnation streamline

C. J. Farrugia,[1] N. V. Erkaev,[2] D. F. Vogl,[3,4] H. K. Biernat,[3,4,5]
M. Oieroset,[6] R. P. Lin,[6] and R. P. Lepping[7]

**Abstract.** We carry out a first comparison with spacecraft measurements of our recent three–dimensional, one–fluid magnetohydrodynamic (MHD) model for the anisotropic magnetosheath [*Erkaev et al.*, 1999], using data acquired by the Wind spacecraft on an inbound magnetosheath pass on December 24, 1994. The spacecraft trajectory was very close to the stagnation streamline, being displaced by less than 1/2 hour from noon and passing at low southern magnetic latitudes (~4.5°). All quantities downstream of the bow shock are obtained by solving the Rankine–Hugoniot equations taking the pressure anisotropy into account. In this application of our model we close the MHD equations by a "bounded anisotropy" ansatz using for this purpose the inverse correlation between the proton temperature anisotropy, $A_p$ ($\equiv T_{p\perp}/T_{p||} - 1$), and the proton plasma beta parallel to the magnetic field $\beta_{p||}$ observed on this pass when conditions are steady. In the model the total perpendicular pressure is prescribed and not obtained self-consistently. For all quantities studied we find very good agreement between the predicted and the observed profiles, indicating that the bounded anisotropy method of closing the magnetosheath equations, first suggested by *Denton et al.* [1994], is valid and reflects the physics of the magnetosheath well. We assess how sensitive our model results are to different parameters in the $A_p = a_0 \beta_{p||}^{-a_1}$ ($a_1 > 0$) relation, taking for $a_1$ the two limiting values (0.4, 0.5) resulting from the two–dimensional hybrid simulations of *Gary et al.* [1997], and varying $a_0$ in the range $0.6 - 0.8$. Input solar wind conditions are as measured on this pass. In general, the model profiles depend more strongly on $a_0$ than on $a_1$. In particular, decreasing $a_0$ narrows the width of the plasma depletion layer (PDL) and widens the mirror stable region. For the lowest value of $a_0$, the mirror stable region extends sunward of the outer edge of the PDL. For the other two values of $a_0$, and regardless of the value of $a_1$, it is contained within the PDL. Finally, we also study phenomenological double-polytropic laws and find polytropic indices $\gamma_\perp \approx 1$ and $\gamma_{||} \approx 1.5$. These results agree well with those of *Hau et al.* [1993] inferred from Active Magnetospheric Particle Tracer Explorers/ Ion Release Module data on a crossing of the near–subsolar magnetosheath.

[1]Institute for the Study of Earth, Oceans, and Space, University of New Hampshire, Durham, New Hampshire, USA.
[2]Institute of Computational Modelling, Russian Academy of Sciences, Krasnoyarsk, Russia.
[3]Space Research Institute, Austrian Academy of Sciences, Graz, Austria.
[4]Also at Institute for Geophysics, Astrophysics, and Meteorology, University of Graz, Graz, Austria.
[5]Also at Institute for Theoretical Physics, University of Graz, Graz, Austria.
[6]Space Science Laboratories, Berkeley, CA, USA.
[7]NASA Goddard Space Flight Center, Greenbelt, MD, USA.



Paper number 2001JA000034.
0148-0227/01/2001JA000034$09.00

## 1. Introduction

The presence of a magnetic field in a plasma introduces temperature anisotropies which can drive various instabilities. The Active Magnetospheric Particle Tracer Explorers (AMPTE) (1984–1986) mission has highlighted the importance of proton temperature anisotropies in the terrestrial magnetosheath, which is typically characterized by $T_{p\perp} > T_{p||}$, where the symbols $\perp$ and $||$ denote directions perpendicular and parallel to the background magnetic field, respectively. The magnetosheath is found to be prone to both the mirror and electromagnetic ion cyclotron wave instabilities, with the value of the proton plasma beta determining which of these two modes dominates the magnetic fluctuation spectrum [e.g., *Fairfield*, 1976; *Crooker and Sis-*

*coe*, 1977; *Tsurutani et al.*, 1982; *Anderson et al.*, 1991; *Phan et al.*, 1994; *Gary*, 1993]. In magnetosheath modeling the question then arises as to the suitable way of closing the anisotropic magnetohydrodynamic (MHD) equations. When the parallel and perpendicular degrees of freedom are energetically decoupled and when the heat flux is negligible, the double adiabatic equations of *Chew et al.* [1956] are appropriate [see, e.g., *Kulsrud*, 1983]. From AMPTE observational work [*Hau et al.*, 1993; *Hill et al.*, 1995] and simulations [*Denton and Lyon*, 1996] it transpires, however, that they are unsuitable for closing the MHD equations in the magnetosheath. Other avenues have to be explored.

AMPTE/Charge Composition Explorer (CCE) investigations have revealed an empirical relation between the proton thermal anisotropy $A_p$ ($\equiv T_{p\perp}/T_{p\|} - 1$) and the plasma beta parallel to the magnetic field $\beta_{p\|}$. Thus, using a set of data pairs $(\beta_{p\|}, A_p)$ measured by the CCE spacecraft in the magnetosheath under compressed conditions necessitated by the low CCE apogee of 8.8 $R_E$, *Anderson and Fuselier* [1993] and *Anderson et al.* [1994] proposed an inverse correlation described by $A_p = 0.85\beta_{p\|}^{-0.48}$ for the magnetosheath plasma downstream of a quasi–perpendicular shock. The physical mechanism giving rise to this relation is that particle scattering in the fluctuating wave fields generated by the anisotropy result in energy transfer from the perpendicular to the parallel directions which inhibits the temperature anisotropy from exceeding an upper bound given by this relation [e.g., *Gary et al.*, 1994]. This empirical relation is consistent with results of linear Vlasov theory, and one– and two–dimensional numerical simulations which for a homogeneous electron–proton plasma and bi–Maxwellian proton velocity distribution functions predict a functional form for the temperature anisotropy of the type $A_p = a_0\beta_{p\|}^{a1}$ [*Gary et al.*, 1994, 1997, and references therein]. A bounded anisotropy fluid model, where the MHD equations are closed by this CCE $A_p(\beta_{p\|})$ relation, has been elaborated by *Denton et al.* [1994] and it has recently been employed in the magnetosheath in one- and two-dimensional simulations (*Denton and Lyon*, 1996, 2000) and in three–dimensional, analytical/numerical models [*Erkaev et al.*, 1999; *Samsonov and Pudovkin*, 2000]. It may be noted that AMPTE/Ion Release Module (IRM) results under less restrictive conditions on the solar wind dynamic pressure predict somewhat different values for parameters $a_0$ and $a_1$, which are also found to depend slightly on the magnetic shear at the magnetopause, and may vary from pass to pass [*Phan et al.*, 1994] (see also discussions of *Denton et al.* [1995], *Gary et al.* [1997], and *Farrugia et al.* [2000]). However, recent two-dimensional hybrid simulations by *Gary et al.* [1997] show that under fairly general conditions, the exponent $a_1$ should lie in the approximate range (0.4, 0.5) for $\beta_{p\|}$ in the range ($\sim 0.05$, $\sim 5$).

In this paper we compare spacecraft observations with the model of *Erkaev et al.* [1999]. In the present application of this analytical/numerical scheme, we close the MHD equations by the relation between $A_p$ and $\beta_{p\|}$ derived specifically from data acquired on this magnetosheath pass when conditions are time steady. The crossing was made on December 24, 1994, by the Wind spacecraft early in its mission. The pass was near the magnetic equator and within 1/2 hour of the noon meridian. The solar wind dynamic pressure was of the order of 4.5 nPa, which corresponds to the lower end of the range of values included in AMPTE/CCE analyses. Aspects of this pass have been discussed by *Phan et al.* [1996], to which reference will be made where appropriate. When we fit model profiles of magnetosheath field and plasma parameters to the measurements we find very good agreement between theory and observations. This agreement shows that the "bounded anisotropy" method of closing the MHD equations in the magnetosheath is valid and reflects well the underlying energy exchange between the parallel and perpendicular degrees of freedom mediated by wave–particle interactions. In view of the recent generalized hybrid code results of *Gary et al.* [1997] mentioned above, we shall then examine from the point of view of our model the effects of different exponents $a_1$ by comparing with results obtained using the two extreme values quoted by Gary et al. [1997]. Parameter $a_0$ is also varied over a range of values obtained in the cited observational work. We can thus gauge how sensitive the model results are to the precise form of the $A_p(\beta_{p\|})$ relation. The results presented here are the first application of our three–dimensional theory of the magnetosheath to spacecraft observations.

## 2. Wind Observations

Data from the Magnetic Field Investigation [*Lepping et al.*, 1995] and the Three-Dimensional Plasma Analyzer [*Lin et al.*, 1995] on the Wind spacecraft for the inbound magnetosheath crossing on December 24, 1994, are shown in Figures 1a and 1b. The panels in Figure 1a display from top to bottom the components of the magnetic field in GSM coordinates, the total field, and the angle $\theta$ between the local magnetic field and the flow velocity. Figure 1b repeats the total field for reference, interpolated to the resolution of the plasma data, and then shows the proton density, temperature, and bulk flow speed, the sum of the magnetic field pressure and the plasma pressure perpendicular to the field ($P_{\mathrm{tot},\perp} = nkT_{p\perp} + B^2/8\pi$), the proton betas, the proton temperature ratio $T_{p\perp}/T_{p\|}$, and, separately, $T_{p\perp}$ and $T_{p\|}$. The plasma data in the magnetosheath and the magnetosphere are from the PESA-H electrostatic analyzer, which measures particles in the energy range 80 eV to 27 keV. These data are not suitable to represent the solar wind, and the data in the solar wind (see below) are as acquired by the Solar Wind Experiment [*Ogilvie et al.*, 1995], also on the Wind spacecraft. The solid lines in the panels will be discussed later (they are

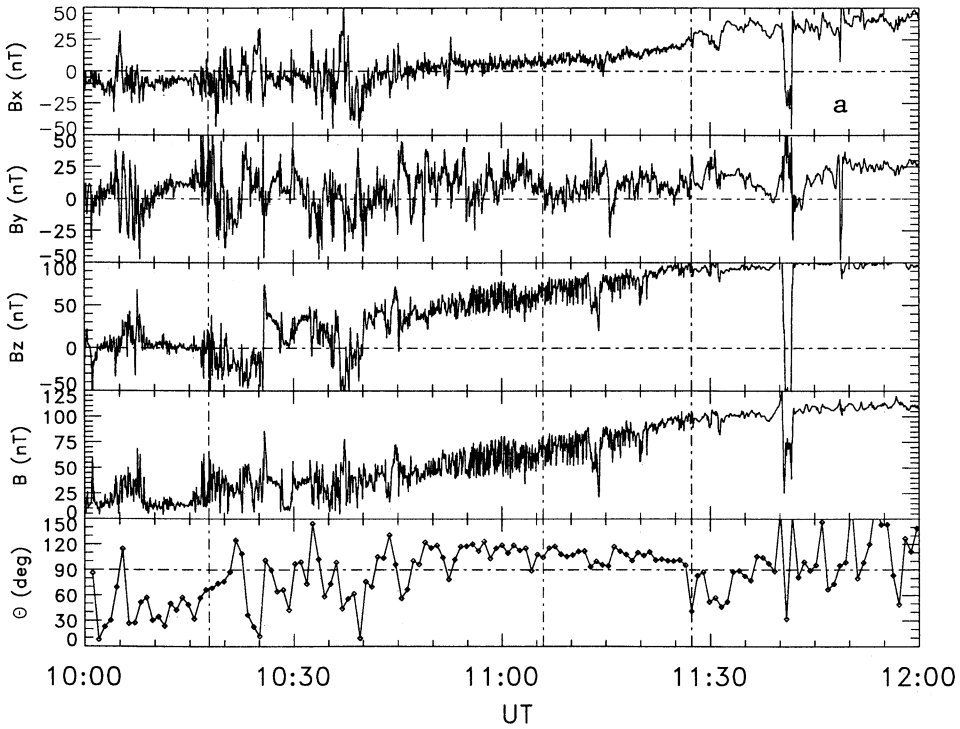


**Figure 1.** Wind data for the inbound magnetosheath pass close to the subsolar streamline on December 24, 1994. From top to bottom the panels show (a) the components of the magnetic field in GSM coordinates, the magnetic field strength, and the angle between the magnetic field and the plasma flow vector and (b) the total field, for reference, the proton density, temperature, and bulk speed, the sum of the magnetic pressure and plasma pressure perpendicular to the background field, the proton betas, the ratio of the perpendicular-to-parallel proton temperatures, and the perpendicular and parallel temperatures. The solid lines in Figure 1b represent modeled variations.

not averages). The temporal resolution of the magnetic field data is 3 s, while that of the proton measurements is ~48 s. Mixed quantities are formed by linearly interpolating the magnetic field quantities to the plasma data resolution. The spacecraft is located at (10.8, -0.1, -0.7) $R_E$ and (7.4, 1.7, -0.8) $R_E$ (GSM coordinates) at 1000 UT and 1200 UT, respectively. With orbital magnetic latitudes and local times of (-4.2°, 12.1 hours) and (-5.4°, 12.5 hours) at the start and end times, Wind's trajectory lies very close to the Sun–Earth line.

Initially, the spacecraft is in the solar wind, crossing first into the magnetosheath at 1017 UT at a radial distance of 10.35 $R_E$ (first vertical guideline). A brief reentry into the solar wind occurs during the time interval 1028 – 1030 UT. The spacecraft enters the magnetosphere at 1127 UT (third vertical guideline) at a radial distance of 8.65 $R_E$. As noted by *Phan et al.* [1996], the local magnetic field rotation across the magnetopause at this crossing is ~5.5°. From previous work [e.g., *Midgley and Davis*, 1963; *Lees*, 1964; *Zwan and Wolf*, 1976; *Paschmann et al.*, 1978, 1993; *Crooker et al.*, 1979; *Erkaev*, 1986; *Phan et al.*, 1994] we expect to find a region adjacent to the sunward side of the magnetopause where the density decreases systematically as the magnetopause is approached and the magnetic field piles up against the magnetopause. Wind observed such a region from 1107 UT to 1127 UT. This is the plasma depletion layer (PDL) and it results from the stretching of magnetic field lines near the magnetospheric obstacle. Assuming stationary conditions to translate time into length scales, this PDL is ~0.6 $R_E$ wide, that is, wider than average [*Paschmann et al.*, 1993]. Wide PDLs result from low solar wind Alfvén Mach numbers [*Farrugia et al.*, 1995, 1997]. Indeed, that the solar wind Alfvén Mach number during this pass is low may be inferred from the relatively modest increases of $B$ and $n$ at the bow shock (from ~15 to 35 nT, and from ~14 to 28 cm$^{-3}$, respectively [Figure 1b, top panels]).

For the anisotropic magnetosheath, we proposed identifying the sunward edge of the PDL as the location where $\beta_{p\|} = 1$ (second vertical guideline [*Erkaev et al.*, 1999; *Farrugia et al.*, 2000]. As Figures 1a and 1b show, the outer location of the PDL (1106 UT) thus defined agrees well with the experimental one based on the behavior of the density and total magnetic field noted above.

After a sharp rise at the bow shock, the density fluctuates around values of 30 cm$^{-3}$ up to ~1045 UT, after which it decreases smoothly toward the magnetopause in the PDL. The trend in the magnetic field strength is generally to increase from ~35 nT just behind the bow shock to ~100 nT at the magnetopause. Assuming

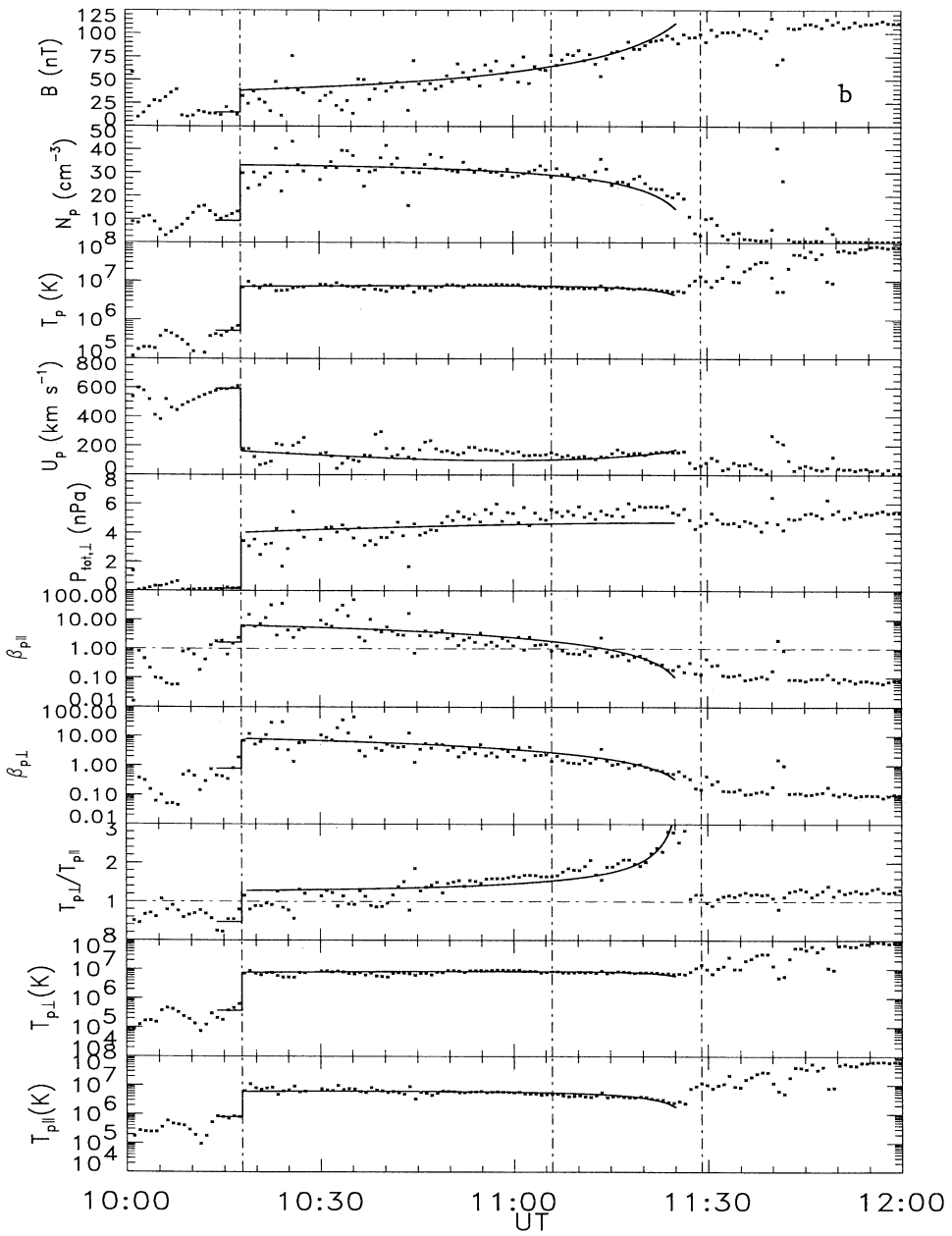


**Figure 1.** (continued)

the magnetopause to be a tangential discontinuity, as is warranted by the low field rotation there and the absence of a jump in the magnetic field strength [*Farrugia et al.*, 1995], we may find the solar wind dynamic pressure $P_{\rm dyn}$ by equating the magnetic pressure of the magnetospheric field just inside the subsolar magnetopause to 0.88 times the solar wind dynamic pressure [*Spreiter et al.*, 1966]. This procedure gives a value of ~4.5 nPa. (Simultaneous solar wind data during this crossing are not available.)

Superposed on the generally increasing trend in the magnetic field strength are large–amplitude ($\delta B/B \sim 0.7$), low–frequency (0.15 Hz) magnetic field fluctuations directed mainly parallel to the background field along the $z$ direction (Figure 1a). These are mirror mode oscillations and, indeed, according to the analysis of *Phan et al.* [1996], the mirror instability criterion is satisfied until ~1114 UT. However, mirror mode oscillations continue until ~1120 UT (Figure 1a). Thus the mirror mode waves inside the PDL on this pass are in part generated locally and in part convected inward with the magnetosheath flow from outside the PDL.

The proton temperature anisotropy $A_p$ increases toward the magnetopause and is evidently anticorrelated with the proton $\beta_{p\parallel}$. Peak anisotropy values reached are moderate, ~1.8 (Figure 1b, last panel). A scatterplot of $A_p$ versus $\beta_{p\parallel}$ for the entire magnetosheath is shown in Figure 2. A least squares fit of the data, shown by the solid line, yielded

$$A_p = 0.67\beta_{p\parallel}^{-0.59}.$$

While this relation fits the region $\beta_{p\parallel} < 4$ well, there is a fair amount of scatter for higher $\beta_{p\parallel}$ val-

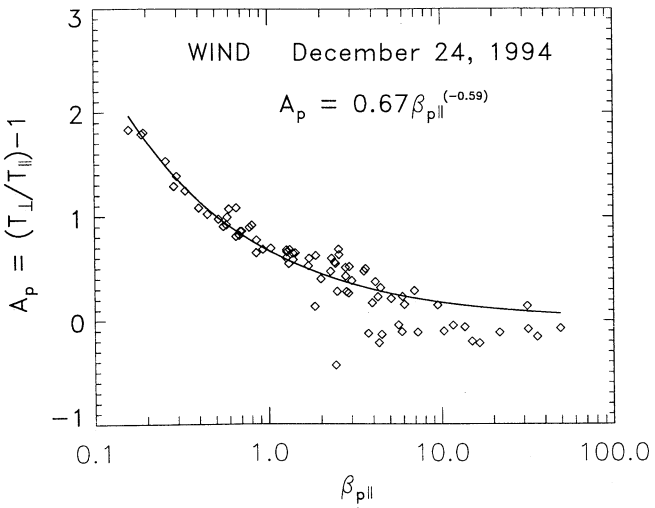


**Figure 2.** A least squares fit of the proton temperature anisotropy $A_p$ and the proton beta parallel to the magnetic field $\beta_{p\|}$ for the entire magnetosheath pass in Figure 1.

ues. The scatter corresponds to the early segment of the pass when nonsteady conditions are evident (for example, Wind encountered the bow shock briefly at ~1028 UT). The flow model we shall discuss below assumes steady state conditions and thus it is appropriate to use the dependence of $A_p$ on $\beta_{p\|}$ from ~1045 to 1127 UT. Least squares fitting gives for this time interval $A_p = 0.73\beta_{p\|}^{-0.50}$. The corresponding $\beta_{p\|}$ range is (0.15, 4). Though we shall obtain model parameters for the whole magnetosheath, we do not expect very good agreement in the early part of the pass.

## 3. Subsolar Anisotropic Magnetosheath: Model Ideas and Results

Our model has been described in detail by *Erkaev et al.* [1999] and we give here only a brief recapitulation to show how the code is implemented in the present example. Jump conditions at the bow shock taking into account the temperature anisotropy are also elaborated.

In our approach we solve the MHD equations for an infinitely conducting, inviscid, dissipationless fluid. These are

$$\rho(\mathbf{u}\cdot\nabla)\mathbf{u} + \nabla\cdot\mathbf{P} + \frac{1}{8\pi}\nabla B^2 - \frac{1}{4\pi}(\mathbf{B}\cdot\nabla)\mathbf{B} = 0, \quad (1)$$

$$\nabla\cdot\left[\rho\mathbf{u}\left(\frac{u^2}{2}+\frac{B^2}{4\pi\rho}+\mathcal{E}\right)+\mathbf{P}\cdot\mathbf{u} - \frac{1}{4\pi}(\mathbf{B}\cdot\mathbf{u})\mathbf{B}\right] = 0, \quad (2)$$

$$\nabla\cdot(\rho\mathbf{u}) = 0, \quad \nabla\times(\mathbf{u}\times\mathbf{B}) = 0, \quad \nabla\cdot\mathbf{B} = 0. \quad (3)$$

Here $\rho$, $\mathbf{u}$, and $\mathbf{B}$ are the mass density, velocity, and magnetic field, respectively. Quantity $\mathbf{P}$ is the pressure tensor, $P_{ik} = P_\perp\delta_{ik} + (P_\| - P_\perp)B_iB_k/B^2$ and $\mathcal{E}$ is the thermal energy, $\mathcal{E} = P_\perp/\rho + 0.5P_\|/\rho$. Equation (1) is the momentum equation; equation (2) expresses the conservation of energy flux, while (3) are the mass continuity equation, the frozen–in magnetic field relation, and the divergence–free condition on the magnetic field, respectively.

Steady state conditions are assumed, and this assumption is consistent with the data, particularly after ~1045 UT [see also *Phan et al.*, 1996]. The equations are closed by relating the plasma pressures by $P_\perp/P_\| = 1 + 0.73\beta_{p\|}^{-0.50}$ derived above. Boundary conditions are specified at the bow shock (see below) and at the magnetopause. The magnetopause is modeled as a tangential discontinuity for which the normal velocity $u_n$ vanishes. The magnetospheric shape is represented by a paraboloid with the Sun–Earth direction as symmetry axis. The solar wind is assumed uniform and its parameters are averages over those measured by Wind in the interval 1013–1018 UT.

To relate quantities upstream and downstream of the bow shock on December 24, 1994, we solve the following jump conditions, expressing various conservation laws under anisotropic pressure conditions [see *Erkaev et al.*, 2000; *Vogl et al.*, 2000]

$$[\![\rho u_n]\!] = 0, \quad (4)$$

$$[\![u_n\mathbf{B}_t - \mathbf{u}_t B_n]\!] = 0, \quad (5)$$

$$\left[\!\!\left[\rho u_n^2 + P_\perp + (P_\| - P_\perp)\frac{B_n^2}{B^2} + \frac{B_t^2}{8\pi}\right]\!\!\right] = 0, \quad (6)$$

$$\left[\!\!\left[\rho u_n\mathbf{u}_t + \frac{B_n\mathbf{B}_t}{4\pi}\left[\frac{4\pi(P_\| - P_\perp)}{B^2} - 1\right]\right]\!\!\right] = 0, \quad (7)$$

$$\left[\!\!\left[\rho u_n\left(\frac{\mathcal{E}}{\rho}+\frac{u^2}{2}+\frac{P_\perp}{\rho}+\frac{B_t^2}{4\pi\rho}\right)+\frac{B_n^2u_n}{B^2}(P_\| - P_\perp) - \frac{(\mathbf{B}_t\cdot\mathbf{u}_t)B_n}{4\pi}\left[1-\frac{4\pi(P_\| - P_\perp)}{B^2}\right]\right]\!\!\right] = 0, \quad (8)$$

$$[\![B_n]\!] = 0. \quad (9)$$

Subscripts $t$ and $n$ denote tangential and normal components to the discontinuity and symbol $[\![Q]\!]$ denotes the jump in quantity $Q$ across the discontinuity.

We consider parameters $A_S$ and $A_M$ which are determined for upstream conditions (subscript 1) by

$$A_M = \frac{1}{M_A^2} \qquad A_S = \frac{P_{\perp 1}}{\rho_1 u_1^2}, \quad (10)$$

where $M_A$ is the Alfvén Mach number ($M_A^2 = 4\pi\rho u^2/B^2$). The components of the magnetic field upstream of the shock are given as $B_{n1} = B_1\cos\theta_{nB}$ and $B_{t1} = B_1\sin\theta_{nB}$, where $\theta_{nB}$ is the angle between the magnetic field vector and the normal vector of the discontinuity. Similarly, the components of the bulk velocity upstream of the shock are chosen as $u_{n1} = u_1\cos\theta_{nu}$ and $u_{t1} = u_1\sin\theta_{nu}$, where $\theta_{nu}$ denotes the angle between the bulk velocity and the normal vector of the shock. We denote the pressure anisotropy $P_\perp/P_\|$ by parameter $\lambda$.

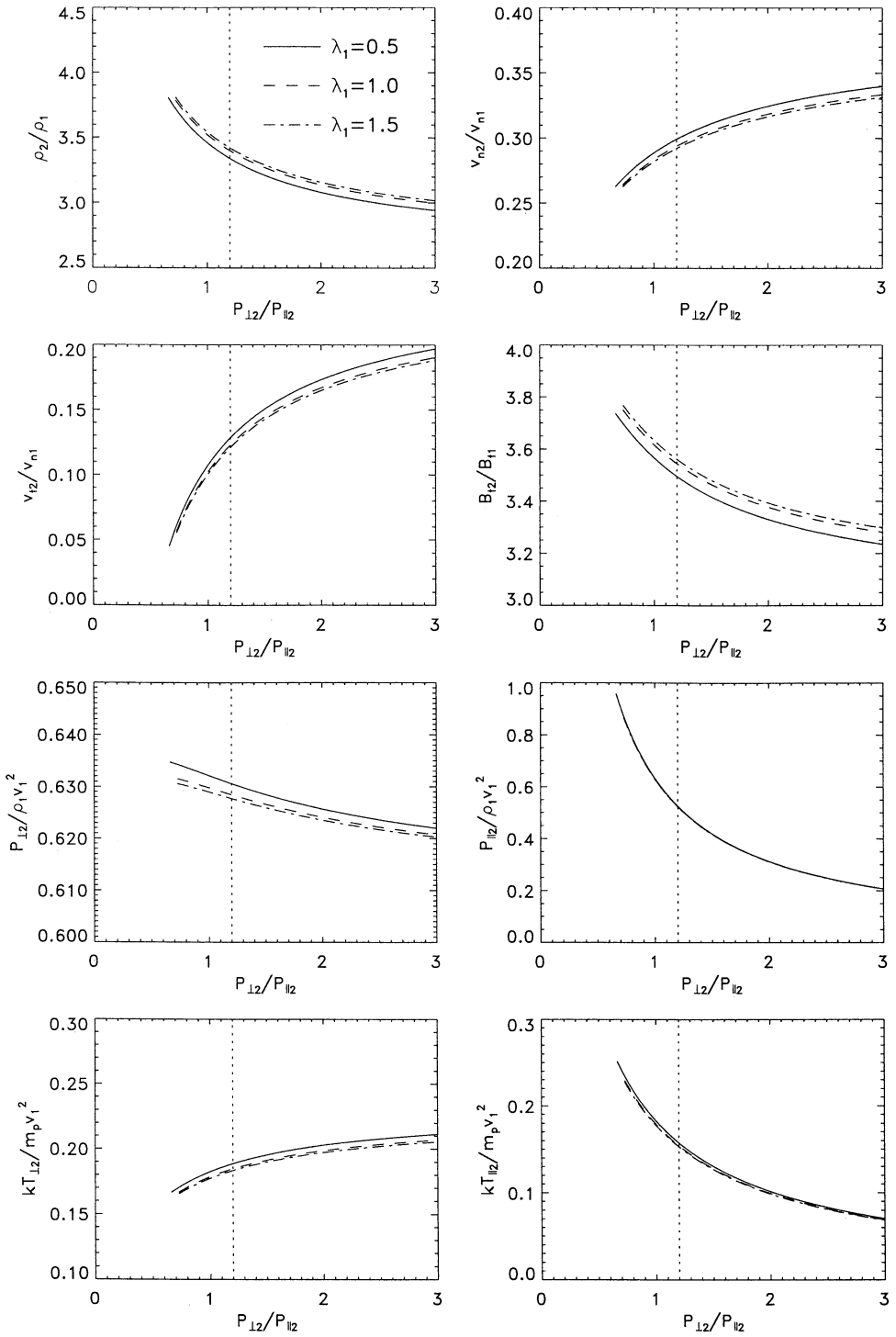


**Figure 3.** Variations of plasma and magnetic field quantities across the bow shock on December 24, 1994, as a function of pressure anisotropy downstream of the shock, $\lambda_2 = P_{\perp 2}/P_{\|2}$. The curves are parameterized by the pressure anisotropy ratio upstream of the shock ($\lambda_1$). For further details, see text.

In order to solve (4)-(9) we introduce the parameters $\varepsilon \equiv 1 - 4\pi(P_{\|2} - P_{\perp 2})/B_2^2$ and $y \equiv \rho_1/\rho_2$, and obtain two equations which have to be solved simultaneously

$$\mathcal{A}_4 y^4 + \mathcal{A}_3 y^3 + \mathcal{A}_2 y^2 + \mathcal{A}_1 y + \mathcal{A}_0 = 0,$$

and

$$\mathcal{D}_3 \varepsilon^3 + \mathcal{D}_2 \varepsilon^2 + \mathcal{D}_1 \varepsilon + \mathcal{D}_0 = 0, \tag{11}$$

where the coefficients are given as

$$\begin{aligned}
\mathcal{A}_4 &= 64\pi^3(1+3\lambda_2), \\
\mathcal{A}_3 &= 16\pi^3 B_{n1}^2(1+2\lambda_2) - 64\pi^3 I_1(1+4\lambda_2) \\
&\quad -16\pi^2 B_{n1}^2 \varepsilon(3+8\lambda_2), \\
\mathcal{A}_2 &= 4\pi B_{n1}^4 \varepsilon[\varepsilon(3+7\lambda_2) - 2(1+2\lambda_2)]
\end{aligned}$$

$$
\begin{aligned}
& +32\pi^2 B_{n1}^2 I_1 \varepsilon(1+4\lambda_2) + 64\pi^3 \lambda_2 (2W_1 - J_1^2), \\
\mathcal{A}_1 &= 8\pi^2 (H_1 + B_{n1} J_1)^2 + B_{n1}^6 \varepsilon^2 (1+2\lambda_2)(1-\varepsilon) \\
& +32\pi^2 B_{n1}^2 \lambda_2 \varepsilon (J_1^2 - 2W_1) \\
& -4\pi B_{n1}^4 I_1 \varepsilon^2 (1+4\lambda_2), \\
\mathcal{A}_0 &= 4\pi B_{n1}^2 \lambda_2 \varepsilon^2 (2B_{n1}^2 W_1 + 2B_{n1} J_1 H_1 + H_1^2), \quad (12) \\
\mathcal{D}_3 &= -B_{n1}^6, \\
\mathcal{D}_2 &= B_{n1}^4 (B_{n1}^2 + 4\pi y(3-\lambda_2) - 4\pi I_1 (1-\lambda_2)), \\
\mathcal{D}_1 &= 16\pi^2 B_{n1}^2 y^2 (2\lambda_2 - 3) + 32\pi^2 B_{n1}^2 y I_1 (1-\lambda_2) \\
& -8\pi B_{n1}^4 y - 16\pi^2 \lambda_2 (J_1 B_{n1} + H_1)^2, \\
\mathcal{D}_0 &= 64\pi^3 y^2 (1-\lambda_2)(y - I_1) + 16\pi^2 B_{n1}^2 y^2 \\
& +8\pi^2 (1+\lambda_2)(J_1 B_{n1} + H_1)^2.
\end{aligned}
$$

Here $H_1$ is the tangential component of the electric field, $I_1$ is the normal component of the momentum flux, $J_1$ is the tangential component of momentum flux, and $W_1$ is the energy flux upstream of the shock,

$$
\begin{aligned}
H_1 &= \sqrt{4\pi A_M} \sin\theta_{nB}, \\
I_1 &= A_S + A_S \cos^2\theta_{nB} \left( \frac{1}{\lambda_1} - 1 \right) \\
& +\frac{1}{2} A_M \sin^2\theta_{nB} + 1, \\
J_1 &= \frac{1}{2} \sin(2\theta_{nB}) \left[ \frac{A_S}{\lambda_1} - A_S - A_M \right], \quad (13) \\
W_1 &= A_S \left( 2 + \frac{1}{2\lambda_1} + \frac{\cos^2\theta_{nB}}{\lambda_1} - \cos^2\theta_{nB} \right) \\
& +A_M \sin^2\theta_{nB} + \frac{1}{2}.
\end{aligned}
$$

Figure 3 shows results for various field and plasma quantities as functions of the pressure anisotropy, $P_{\perp 2}/P_{\parallel 2} = \lambda_2$, downstream of the shock, for fixed solar wind parameters obtained from the data on December 24, 1994; $A_S = 0.012$, $A_M = 0.026$, $\theta_{nB} = 52.2°$, and $\theta_{nu} = 3.9°$. The three curves in each panel are parameterized by three different values of $\lambda_1$ (= 0.5, 1.0, 1.5). From top to bottom are plotted the variations of the plasma density, the normal and tangential components of the velocity, the tangential component of the magnetic field strength, and the pressures and temperatures perpendicular and parallel to the magnetic field. The vertical dashed line indicates the value for each parameter immediately downstream of the bow shock on December 24, 1994, which will be used as boundary condition on the model described below. All parameters are monotonic functions of the anisotropy rate $\lambda_2$. All have only a weak dependence on the anisotropy in the solar wind $\lambda_1$.

Next we discuss the magnetosheath model of *Erkaev et al.* [1999]. To integrate the MHD equations, we stipulate the variation of the total perpendicular pressure along and perpendicular to the magnetopause. Along the magnetopause we assume a Newtonian variation, that is, $P_{\mathrm{tot},\perp,\mathrm{m}} = (P_{\mathrm{tot},\perp,0} - P_{\mathrm{tot},\perp,\infty}) \cos^2\theta + P_{\mathrm{tot},\perp,\infty}$, where $P_{\mathrm{tot},\perp,\mathrm{m}}$ is the total perpendicular pressure at a given point $R$ on the magnetopause and $P_{\mathrm{tot},\perp,0}$ and $P_{\mathrm{tot},\perp,\infty}$ are the total perpendicular pressures at the stagnation point on the magnetopause and upstream of the bow shock, respectively. Parameter $\theta$ is the angle between the normal to the magnetopause at point $R$ and the stagnation streamline. This is the preferred form for this pressure variation as given by *Petrinec and Russell* [1997] review. For the variation of the total perpendicular pressure $P_{\mathrm{tot},\perp}$ with distance $\mu$ from the magnetopause along the normal, we have in past work used a quadratic variation, that is, we have assumed

$$
P_{\mathrm{tot},\perp} = P_{\mathrm{tot},\perp,\mathrm{m}} (1 - \mu^2/\delta^2) + P_{\mathrm{tot},\perp,\mathrm{s}} \mu^2/\delta^2,
$$

where $\delta$ is the magnetosheath thickness and $P_{\mathrm{tot},\perp,\mathrm{m}}$ and $P_{\mathrm{tot},\perp,\mathrm{s}}$ are, respectively, the perpendicular pressures at the magnetopause and immediately downstream of the bow shock derived from the model. Experience with data suggests that this specific functional form models the variation of $P_{\mathrm{tot},\perp}$ well. Its validity is checked against the observations a posteriori. Note, however, that by prescribing, rather than obtaining, $P_{\mathrm{tot},\perp}$, the model is not self-consistent.

Before integrating, the MHD equations are transformed twice. First, they are written as "magnetic string" equations via a transformation from Cartesian to frozen-in coordinates [*Pudovkin and Semenov*, 1977]. (Magnetic string equations are so called because of a formal analogy with the equations of a vibrating string. The string here is a magnetic field line loaded with plasma.) Second, these equations are expressed in body coordinates [see *Erkaev et al.*, 1999, equations (26) – (34)]. Details of the numerical integration procedure are given by *Erkaev et al.* [1999].

A map of the magnetic field lines (dashed) and flow streamlines (solid) in the vicinity of the magnetopause, obtained from the numerical solution, is shown in Figure 4. The spatial unit in this figure is the curvature ratio of the magnetosphere at the subsolar point. The view is from the Sun. The subsolar point is at the center. One can see that away from the subsolar region the flow streamlines become almost perpendicular to the magnetic field lines. This is stagnation line flow. It may be seen that the magnetic field lines converge near dawn and dusk. This is a real effect and is due to the following. The frozen-in magnetic field lines drape around the dayside magnetopause, and they converge asymptotically as we recede from the subsolar point along the interplanetary magnetic field (IMF) direction. The central part of the field line (dashed) shown in the figure is closest to the magnetosphere. It moves rapidly with the accelerated plasma flow in the direction perpendicular to the magnetic field. The acceleration of the plasma flow is caused by a strong magnetic field tension near the magnetopause. However, on the flanks the field line is far away from the magnetopause and it thus moves rather slowly in the direction perpendicular to the magnetic field.

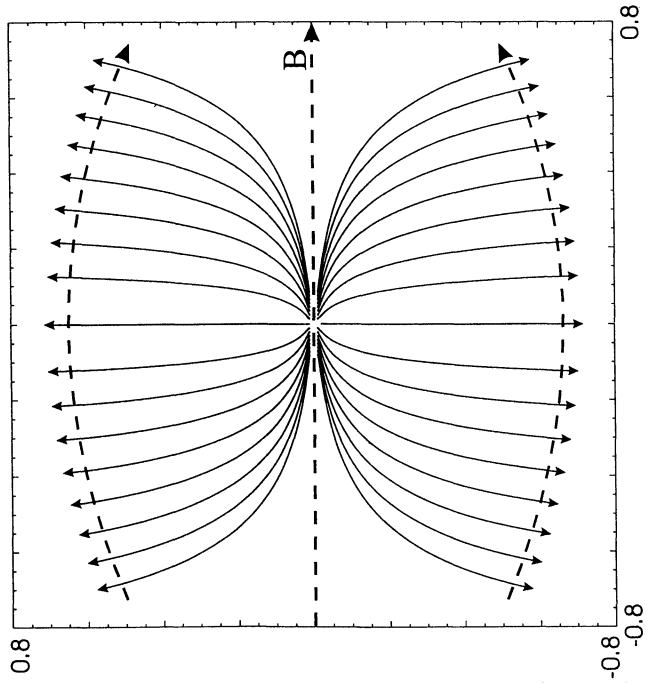


**Figure 4.** The pattern of magnetic field lines (dashed) and flow streamlines near the dayside magnetopause computed by our model. The view is from the Sun.

The model results for various magnetosheath quantities are shown by solid lines in Figure 1b. The input solar wind parameters are the averages shown by short horizontal lines in each panel before the spacecraft first crosses the bow shock. It is evident that the time series of all parameters are reproduced well by the model, particularly after the large fluctuations in the high beta regime in the outer magnetosheath subside and more steady conditions prevail. Thus the oppositely directed changes in $B$ and $n$ in the PDL are also present in the theoretical variations, and the modeled degree of depletion is similar to that observed. The predicted bulk speed profile also has the (small) increase in the PDL resulting from plasma acceleration in the stagnation line flow pattern at the low-shear magnetopause [*Sonnerup*, 1974; *Phan et al.*, 1994]. The modeled temperature ratio, after the interval 1015–1045 UT where it overestimates the measurements, follows the observations closely. The modeled $T_{p\perp}/T_{p\|}$ ratio increases primarily as a result of a decrease in $T_{p\|}$; the modeled $T_{p\perp}$ component is nearly constant up to the magnetopause (last two panels). Similar behavior is seen in the data on this pass and is common to other magnetosheath data sets in the PDL region (see, e.g., the superposed epoch analysis profiles of *Phan et al.* [1994].

## 4. Discussion and Conclusions

In this paper we have reported the first comparison of our ideal MHD model incorporating anisotropic pressures ($P_\perp > P_\|$) with spacecraft data in a magnetosheath traversal very close to the flow stagnation streamline. In line with recent theorizing and simulation work, we have closed the equations by an empirical relation derived from data on this pass relating the proton temperature anisotropy and the proton plasma beta parallel to the magnetic field. The physical meaning of this bounded anisotropy condition is as follows: The temperature anisotropy acts as a macroscopic driver of plasma instabilities and the wave–particle interactions in the associated field fluctuations redistribute the energy and thus limit the anisotropy to remain at this bound.

The evident agreement between modeled and observed magnetosheath quantities, particularly at those times where the data suggest that the steady conditions presupposed by the model actually prevail, lends confidence in the correctness of the algorithm and in the use of empirically derived $A_p(\beta_{p\|})$ relations as closure relations for the magnetosheath plasma.

Figure 5 plots the $(T_{p\perp}/T_{p\|}) - 1 - (1/\beta_{p\perp})$ as a function of UT in the magnetosheath. A value of zero corresponds to the threshold condition for the mirror instability in the limit of zero growth. It is seen that from 1045 to 1115 UT the magnetosheath is continuously mirror unstable, with positive growth. On this pass this corresponds to the range of $\beta_{p\|} = (\sim 3, \sim 0.6)$. Thus while statistically the magnetosheath is generally considered to be marginally mirror unstable [*Hill et al.*, 1995; *Phan et al.*, 1994], it may have positive growth over large segments on individual passes like this one.

In extensive IRM and CCE data and theoretical investigations over the last decade, various $A_p(\beta_{p\|})$ relations of the functional form $A_p = a_0\beta_{p\|}^{-a_1}$ have been proposed, with the different parameters reflecting partly the local and partly the solar wind conditions under which the measurements were made. Thus, under elevated solar wind dynamic pressure, AMPTE/CCE measurements behind quasi-perpendicular and quasi-parallel shocks may be summarized by $a_0 = 0.85, a_1 = 0.48$ [*Anderson et al.*, 1994], and $a_0 = 0.83, a_1 = 0.58$ [*Fuselier et al.*, 1994], respectively. AMPTE/IRM re-

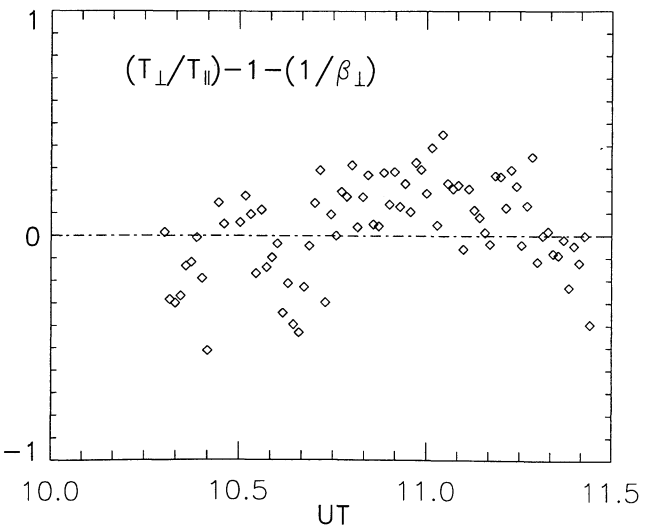


**Figure 5.** A plot of the threshold condition of the mirror instability (zero growth) as a function of UT.

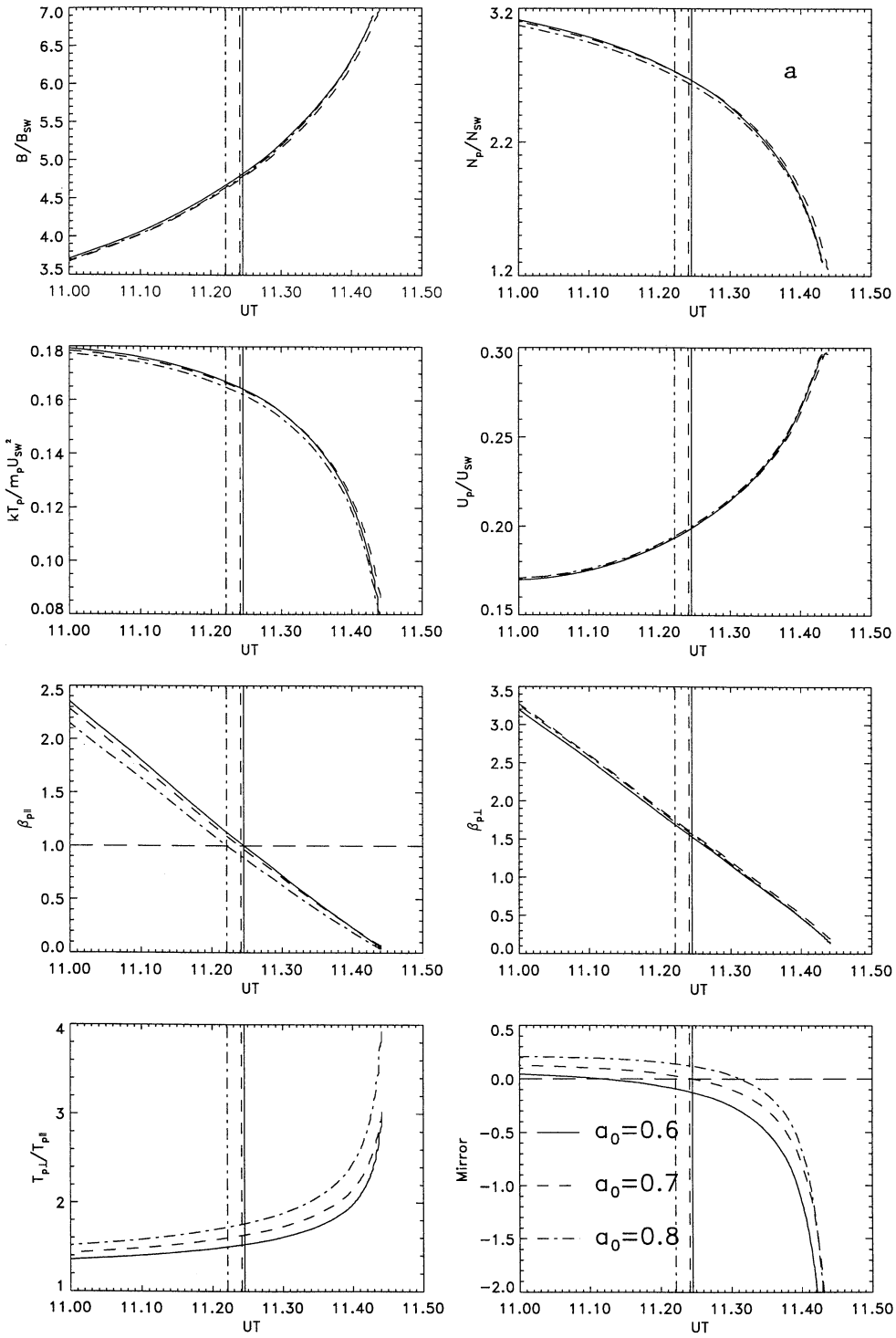


**Figure 6.** Quantities $B$, $N_p$, $T_p$, $U_p$, $\beta_{p\|}$, $\beta_{p\perp}$, $T_{p\perp}/T_{p\|}$, and the criterion of the mirror instability calculated by the model for two limiting values of the exponent $a_1$ in the $A_p(\beta_{p\|})$ relation: (a) $a_1 = 0.4$ and (b) $a_1 = 0.5$. The same input solar wind conditions as observed by Wind on December 24, 1994, are used. For each quantity, three curves are shown corresponding to $a_0 = 0.6$, 0.7, and 0.8, respectively.

sults, which are more extensive and less constrained by the solar wind dynamic pressure, gave for low–shear and high–shear passes, respectively, the fitted pairs of coefficients $a_0 = 0.63, a_1 = 0.50$, and $a_0 = 0.54, a_1 = 0.47$ [*Phan et al.*, 1994].

Examining the question of the magnetosheath anisotropy upper bound by two–dimensional hybrid simulations, *Gary et al.* [1997] found that (1) coefficient $a_0$ is of the order of 1 but its exact value depends on the anisotropy rate, the composition of the magnetosheath plasma, and the presence of a cold $H^+$ component, and thus can be quite variable; and (2) for a value of the

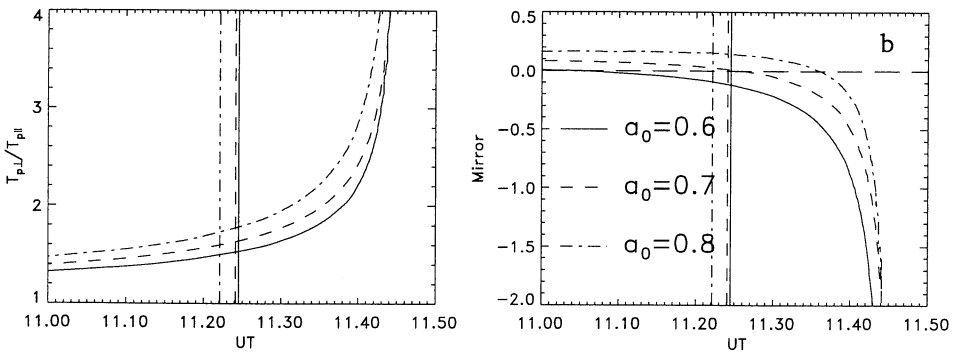


**Figure 6.** (continued)

proton $\beta_{p\parallel}$ in the approximate range (0.05, 5), exponent $a_1$ should vary within the range [~0.4, ~0.5] in anisotropic homogeneous plasmas characterized by bi-Maxwellian hot distribution functions. We now wish to examine from the point of view of our model what differences would result with the data for the two extreme values of $a_1$ predicted by *Gary et al.* [1997]. For each value of $a_1$ we compute model profiles for three values of $a_0$ (= 0.6, 0.7, 0.8). The results for $a_0 = 0.7$, $a_1 = 0.50$ correspond to nominal values obtained in this case and results have been shown already in Figure 1b. For the total magnetosheath profiles (not shown), trends are qualitatively similar to Figure 1b for all values of $a_0$ and $a_1$. Quantitative differences in corresponding individual profiles are small. In particular, the main body of the magnetosheath is mirror unstable in all parameter variations, with the highest growth rates occurring for the largest $a_0$ and the lower $a_1$.

We now focus on the inner magnetosheath. In Figure 6a we plot from top to bottom $B$, $N_p$, $T_p$, $U_p$, $\beta_{p\parallel}$, $\beta_{p\perp}$, $T_{p\perp}/T_{p\parallel}$ and the mirror criterion. In Figure 6b we only show $T_{p\perp}/T_{p\parallel}$ and the mirror criterion. Figures 6a and 6b refer to $a_1 = 0.4$ and 0.5, respectively. (Note that the UT on the horizontal axes is given in decimal hours.) The vertical guidelines indicate the location of $\beta_{p\parallel} = 1$ for each value of $a_0$, moving earthward (to the right) as $a_0$ decreases.

It can be seen that the model results are not very sensitive to the assumed variations of parameters $a_0$ and $a_1$. The only sizeable difference occurs in $\beta_{p\parallel}$ (which determines in our model the outer edge of the PDL), the modeled $T_{p\perp}/T_{p\parallel}$ ratio, and the mirror threshold criterion for zero growth. The modeled temperature anisotropy is highest for the largest value of $a_0$. While the influence of $a_1$ on the PDL position is insignificant, PDL width decreases substantially with $a_0$. The mirror stable region is widest for $a_0 = 0.6$ and $a_1 = 0.5$, and it is narrowest for $a_0 = 0.8$ and $a_1 = 0.5$. Thus decreasing parameter $a_0$ makes the mirror stable region wider. A comparison of the relative widths of the mirror stable region and the PDL for different $a_0$ shows that for the lowest value of $a_0$ and both values of $a_1$, the mirror stable region extends sunward of the PDL outer edge. For the other two values of $a_0$ it is either coextensive with the PDL ($a_0 = 0.7$) or is contained well within the PDL. In the latter case therefore the outer part of the PDL is still locally mirror unstable.

In an alternative approach to the modeling of the thermodynamics of the anisotropic magnetosheath plasma, *Hau and Sonnerup* [1993] developed a phenomenological approach based on double-polytropic closure. These are polytropic laws of the form $P_\perp/\rho B^{\gamma_\perp - 1} = C_\perp$, and $P_\parallel B^{\gamma_\parallel - 1}/\rho^{\gamma_\parallel} = C_\parallel$. (The double adiabatic equations of *Chew et al.* [1956] are a special case for which $\gamma_\perp = 2$, and $\gamma_\parallel = 3$.) Subsequently, *Hau et al.* [1993] applied this formalism to a set of 29 crossings of the dayside magnetosheath made by the IRM spacecraft and found $\gamma_\perp$ and $\gamma_\parallel$ to lie typically in the ranges 0.94 ± 0.10 and 1.14 ±0.13, respectively. These passes were spread over 6 hours in local time range (8–14 hours) and had magnetic latitudes $\leq 30°$. They included both low and high shear cases [*Hau et al.*, 1993]. A case event study was also made for the IRM pass on October 24, 1985, which being at comparable southern latitudes and an average of only 1.5 hours postnoon, bears comparison with the Wind pass on December 24, 1994. For the October 24, 1985, pass, *Hau et al.* [1993] derive the following polytropic indices for the protons: $\gamma_\perp = 0.83$ and $\gamma_\parallel = 1.47$. They thus conclude that in the direction perpendicular to the field the behavior of the protons approximates the isothermal limit. *Hau et al.* [1993] then studied theoretical predictions for the dependence of $T_{p\perp}/T_{p\parallel}$ on $\beta_{p\parallel}$, considering three models: (1) the mirror stability threshold; (2) the $A_p(\beta_{p\parallel})$ relation derived from CCE data, $A_p = 0.85\beta_{p\parallel}^{-0.48}$; and (3) the polytropic approximation. They concluded that the quality of agreement with data of model 3 was comparable to that of model 2.

We attempt a similar treatment for December 24, 1994. Figure 7 shows the result of a least squares fit to polytropic expressions in the perpendicular (top panel) and parallel (bottom panel) directions. Normalization of polytropes was done by dividing by their average values, so that optimal agreement is achieved when $C_\perp = C_\parallel = 1$. Parameters $\gamma_\perp$ and $\gamma_\parallel$ were fitted to be 1.04

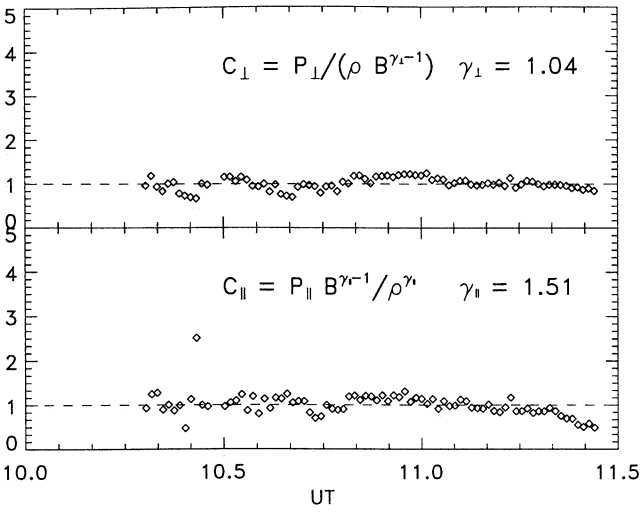


**Figure 7.** Least squares fits of polytropes normalized to their average value over all the magnetosheath measurements for the (top) perpendicular and (bottom) parallel pressures. The fitted values of the polytropic indices are $\gamma_\perp = 1.04$ and $\gamma_{||} = 1.51$.

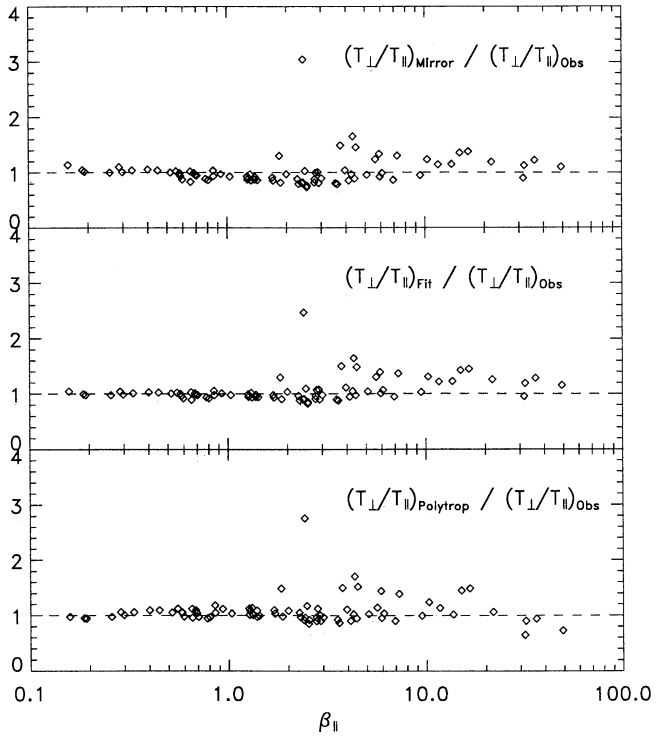


**Figure 8.** The $T_{p\perp}/T_{p||}$ ratios predicted by three models: (top) mirror instability, (middle) empirical $A_p(\beta_{p||})$ fit, and (bottom) double polytropic fits. The measurements are normalized by the observed values.

and 1.51, respectively. The level of agreement with the data is seen to be quite good except in the parallel pressure close to the magnetopause. The sums of residues are 1.44 and 2.68, for the perpendicular and parallel polytropes, respectively. In both studies therefore the perpendicular pressure obeys an isothermal law reasonably well, while in the parallel direction, the polytropic indices are of the order of 1.5 in both studies. The results of *Hau et al.* [1993] and this study suggest that the thermodynamics of the magnetosheath plasma in the subsolar region may be described reasonably well

$$P_\perp/\rho = C_\perp, \quad P_{||}B^{1/2}/\rho^{1.5} = C_{||}.$$

Figure 8 shows the temperature ratio normalized to the observed values for the three theoretical approaches. From top to bottom the points show the ratio from the marginal mirror instability criterion, from the empirical $A_p(\beta_{p||})$ of Figure 2, and finally from the polytropic laws. It can be seen that the polytropic values are comparable in quality to that of the empirical fit. The sum of squares $S$ is however least for the empirical fit in the middle panel ($S$=4.56 versus $S$=6.69 (marginal mirror instability) and $S$=5.84 (polytropes)).

In conclusion, we have shown that our anisotropic magnetosheath flow model with an $A_p(\beta_{p||})$ closure relation derived from data on the pass examined can account for the observations well. It is desirable to study other passes to further confirm this conclusion. We have studied how sensitive our results are to variations of the coefficients in the $A_p(\beta_{p||})$ relation using values typical of those quoted in the literature. The double polytropic approach, though phenomenological in nature, does appear to suggest that near the subsolar region the protons obey double polytropic laws of indices 1 and 1.5 in the perpendicular and parallel direction, respectively. This last point confirms the original work of *Hau et al.* [1993].

**Acknowledgments.** Part of this work was done while C.J.F. and N.V.E. were on a research visit to the Space Research Institute of the Austrian Academy of Sciences in Graz, and D.F.V. was on a research visit to the Institute for the Study of Earth, Oceans, and Space of the University of New Hampshire. This work is supported by NASA grant NAG5–2834, by NASA Living with a Star grant NAG5–10883, by the INTAS–ESA project 99–01277, by grant 01–05–02003, grant 01–05–65070 from the Russian Foundation of Basic Research, by grant 97–0–13.0–71 from the Russian Ministry of Education, by the Austrian "Fonds zur Förderung der wissenschaftlichen Forschung" under project P12761–TPH, and by project No I.4/2001 from "Österreichischer Akademischer Austauschdienst". We acknowledge support by the Austrian Academy of Sciences, "Verwaltungsstelle für Auslandsbeziehungen".

Janet G. Luhmann thanks S. Peter Gary and other referees for their assistance in evaluating this paper.

## References

Anderson, B. J., and S. A. Fuselier, Magnetic pulsations from 0.1 to 4.0 Hz and associated plasma properties in the Earth's subsolar magnetosheath and plasma depletion layer, *J. Geophys. Res., 98*, 1461, 1993.

Anderson, B. J., S. A. Fuselier, and D. Murr, Electromagnetic ion cyclotron waves in the plasma depletion layer, *Geophys. Res. Lett., 18*, 1955, 1991.

Anderson, B. J., S. A. Fuselier, S. P. Gary, and R. E. Denton, Magnetic spectral signatures in the Earth's magnetosheath and plasma depletion layer, *J. Geophys. Res., 99,* 5877, 1994.

Chew, G. F., M. L. Goldberger, and F. E. Low, The Boltzmann equation and the one-fluid hydromagnetic equations in the absence of particle collisions, *Proc. R. Soc. London A, 236,* 112, 1956.

Crooker, N. U., and G. L. Siscoe, A mechanism for pressure anisotropy and mirror instability in the dayside magnetosheath, *J. Geophys. Res., 82,* 185, 1977.

Crooker, N. U., T. E. Eastman, and G. S. Stiles, Observations of plasma depletion in the magnetosheath at the magnetopause, *J. Geophys. Res., 84,* 869, 1979.

Denton, R. E., and J. G. Lyon, Density depletion in an anisotropic magnetosheath, *Geophys. Res. Lett., 23,* 2891, 1996.

Denton, R. E., and J. G. Lyon, Effect of pressure anisotropy on the structure of a two-dimensional magnetosheath, *J. Geophys. Res., 105,* 7545, 2000.

Denton, R. E., B. J. Anderson, S. P. Gary, and S. A. Fuselier, Bounded anisotropy fluid model for ion temperatures, *J. Geophys. Res., 99,* 11,225, 1994.

Denton, R. E., X. Li, and T.-D. Phan, Bounded anisotropy fluid model for ion temperature evolution applied to AMPTE/IRM magnetosheath data, *J. Geophys. Res., 100,* 14,925, 1995.

Erkaev, N. V., The results of study of MHD flow around the magnetosphere, *Geomagn. Aeron., 26,* 595, 1986.

Erkaev, N. V., C. J. Farrugia, and H. K. Biernat, Three-dimensional, one-fluid, ideal MHD model of magnetosheath flow with anisotropic pressure, *J. Geophys. Res., 104,* 6877, 1999.

Erkaev, N. V., D. F. Vogl, and H. K. Biernat, Solution of jump conditions for fast shocks in anisotropic magnetized plasma, *J. Plasma Phys., 64,* 561, 2000.

Fairfield, D. H., Waves in the vicinity of the magnetopause, in *Magnetospheric Particles and Fields*, edited by B. M. Mc Cormac, 67 pp., D. Reidel, Norwell, Mass., 1976.

Farrugia, C. J., N. V. Erkaev, H. K. Biernat, and L. F. Burlaga, Anomalous magnetosheath properties during passage of an interplanetary magnetic cloud, *J. Geophys. Res., 100,* 19,245, 1995.

Farrugia, C. J., N. V. Erkaev, H. K. Biernat, G. R. Lawrence, and R. C. Elphic, Plasma depletion layer for low solar wind Alfvén Mach numbers: Comparison with ISEE observations, *J. Geophys. Res., 102,* 11,315, 1997.

Farrugia, C. J., N. V. Erkaev, and H. K. Biernat, On the effects of solar wind dynamic pressure on the anisotropic terrestrial magnetosheath, *J. Geophys. Res., 105,* 115, 2000.

Fuselier, S. A., B. J. Anderson, S. P. Gary, and R. E. Denton, Inverse correlations between the ion temperature anisotropy and plasma beta in the Earth's quasi-parallel magnetosheath, *J. Geophys. Res., 99,* 14,931, 1994.

Gary, S. P., *Theory of Space Plasma Microinstabilities*, Cambridge Univ. Press, New York, 1993.

Gary, S. P., B. J. Anderson, R. E. Denton, S. A. Fuselier, and M. E. McKean, A limited closure relation for anisotropic plasmas in the Earth's magnetosheath, *Phys. Plasmas, 1,* 1676, 1994.

Gary, S. P., J. Wang, D. Winske, and S. A. Fuselier, Proton temperature anisotropy upper bound, *J. Geophys. Res., 102,* 17,159, 1997.

Hau, L.-N., and B. U. Ö. Sonnerup, On slow-mode waves in an anisotropic plasma, *Geophys. Res. Lett., 20,* 1763, 1993.

Hau, L.-N. , T.-D. Phan, B. U. O. Sonnerup, and G. Paschmann, Double polytropic closure in the magnetosheath, *Geophys. Res. Lett., 20,* 2255, 1993.

Hill, P., G. Paschmann, R. A. Treumann, W. Baumjohann, and N. Sckopke, Plasma and magnetic field behavior across the magnetosheath near local noon, *J. Geophys. Res., 100,* 9575, 1995.

Kulsrud, R. M., MHD description of plasma, in *Handbook of Plasma Physics*, vol. 1, edited by A. A. Galeev, and R. N. Sudan, p. 115, North-Holland, New York, 1983.

Lees, L., Interaction between the solar wind plasma and the geomagnetic cavity, *AIAA J., 2,* 1576, 1964.

Lepping, R. P., et al., The Wind magnetic field investigation, *Space Sci. Rev., 71,* 207, 1995.

Lin, R. P., et al., A three-dimensional plasma and energetic particle investigation for the Wind spacecraft, *Space Sci. Rev., 71,* 125, 1995.

Midgley, J. E., and L. Davis, Calculation by a moment technique of the perturbation of the geomagnetic field by the solar wind, *J. Geophys. Res., 68,* 5111, 1963.

Ogilvie, K. W., et al., SWE, A comprehensive plasma instrument for the Wind spacecraft, *Space Sci. Rev., 71,* 55, 1995.

Paschmann, G., N. Sckopke, G. Haerendel, I. Papamastorakis, S. J. Bame, J. R. Asbridge, J. T. Gosling, E. W. Hones Jr., and E. T. Tech, ISEE plasma observations near the subsolar magnetopause, *Space Sci. Rev., 22,* 717, 1978.

Paschmann, G., W. Baumjohann, N. Sckopke, T.-D. Phan, and H. Lühr, Structure of the dayside magnetopause for low magnetic shear, *J. Geophys. Res., 98,* 13,409, 1993.

Petrinec, S. M., and C. T. Russell, Hydrodynamics and MHD equations across the bow shock and along the surfaces of planetary obstacles, *Space Sci. Rev., 79,* 757, 1997.

Phan, T.-D., G. Paschmann, W. Baumjohann, N. Sckopke, and H. Lühr, The magnetosheath region adjacent to the dayside magnetopause: AMPTE/IRM observations, *J. Geophys. Res., 99,* 121, 1994.

Phan, T.-D., et al., The subsolar magnetosheath and magnetopause for high solar wind ram pressure: Wind observations, *Geophys. Res. Lett., 23,* 1279, 1996.

Pudovkin, M. I., and V. S. Semenov, Stationary frozen-in coordinate system, *Ann. Geophys., 33,* 429, 1977.

Samsonov, A. A., and M. I. Pudovkin, Application of the bounded anisotropy model for the dayside magnetosheath, *J. Geophys. Res., 105,* 12,859, 2000.

Sonnerup, B. U. Ö., The reconnecting magnetosphere, in *Magnetosphere Physics*, edited by B. M. McCormac, p. 23, D. Reidel, Norwell, Mass., 1974.

Spreiter, J. R., A. L. Summers, and A. Y. Alksne, Hydromagnetic flow around the magnetosphere, *Planet. Space Sci., 14,* 223, 1966.

Tsurutani, B. T., E. J. Smith, R. R. Anderson, K. W. Ogilvie, J. D. Scudder, D. N. Baker, and S. J. Bame, Lion roars and nonoscillatory drift mirror waves in the magnetosheath, *J. Geophys. Res., 87,* 6060, 1982.

Vogl, D. F., H. K. Biernat, N. V. Erkaev, C. J. Farrugia, and S. Mühlbachler, Jump conditions for pressure anisotropy, and comparison with the Earth's bow shock, *Nonlinear Proc. Geophys., 8,* 167, 2000.

Zwan, B. J., and R. A. Wolf, Depletion of solar wind plasma near a planetary boundary, *J. Geophys. Res.*, *81*, 1636, 1976.

---

H. K. Biernat and D. F. Vogl, Space Research Institute, Austrian Academy of Sciences, Schmiedlstrasse 6, A–8042 Graz, Austria.

N. V. Erkaev, Institute of Computational Modelling, Russian Academy of Sciences, 660036, Krasnoyarsk, Russia.

C. J. Farrugia, Institute for the Study of Earth, Oceans, and Space, Space Science Center, University of New Hampshire, Morse Hall, Room 414, 39 College Road, Durham, NH 03824-3525, USA. (charlie.farrugia@unh.edu, roy.torbert@unh.edu)

R. P. Lepping, NASA Goddard Space Flight Center, Greenbelt, MD 20771, USA.

R. P. Lin and M. Oieroset, Space Science Laboratories, University of California, Berkeley, CA 94720, USA.

(Received January 31, 2001; revised August 28, 2001; accepted August 29, 2001.)